

**Orbital magnetic moments of oxygen and chromium in CrO<sub>2</sub>**D. J. Huang,<sup>1</sup> H.-T. Jeng,<sup>2</sup> C. F. Chang,<sup>1</sup> G. Y. Guo,<sup>3,1</sup> J. Chen,<sup>4,1</sup> W. P. Wu,<sup>5,1</sup> S. C. Chung,<sup>1</sup>  
S. G. Shyu,<sup>6,7</sup> C. C. Wu,<sup>6</sup> H.-J. Lin,<sup>1</sup> and C. T. Chen<sup>1,3</sup><sup>1</sup>*Synchrotron Radiation Research Center, Hsinchu 300, Taiwan*<sup>2</sup>*Physics Division, National Center for Theoretical Sciences, Hsinchu 300, Taiwan*<sup>3</sup>*Department of Physics, National Taiwan University, Taipei 106, Taiwan*<sup>4</sup>*Department of Physics, National Chung Cheng University, Chia-Yi 621, Taiwan*<sup>5</sup>*Department of Electrophysics, National Chiao-Tung University, Hsinchu 300, Taiwan*<sup>6</sup>*Institute of Chemistry, Academia Sinica, Nankang, Taipei 115, Taiwan*<sup>7</sup>*Department of Chemistry, National Central University, Tao-Yuan 320, Taiwan*

(Received 25 March 2002; revised manuscript received 19 August 2002; published 27 November 2002)

With measurements of the magnetic circular dichroism and band-structure calculations in the local spin density approximation (LSDA+U) approach, we revealed that the orbital moment of O in CrO<sub>2</sub> is ferromagnetically coupled to that of Cr, whereas the spin moment of O is antiferromagnetically coupled to that of Cr. Spin and orbital magnetic moments of Cr and O are enhanced as Coulomb interaction energy  $U$  increases. Comparing the magnetic circular dichroism data with the LSDA+U calculations, we conclude that it is essential to include the on-site Coulomb energy for adequately describing the orbital magnetic moments of CrO<sub>2</sub>.

DOI: 10.1103/PhysRevB.66.174440

PACS number(s): 75.50.Ss, 71.28.+d, 75.25.+z, 78.70.Dm

Transition-metal oxides, which are interesting for fundamental research and important for technological applications, exhibit anomalous and interesting physical properties.<sup>1</sup> These interesting properties are determined by a coupling between the charge, orbital characters, and spin of the valence electrons, and the lattice degrees of freedom in transition-metal oxides. For instance, magnetic oxides such as manganates and CrO<sub>2</sub> have drawn much attention because of their colossal magnetoresistance and half-metallic behavior. The orbital magnetism, a consequence of this coupling mediated by spin-orbit interactions, of these materials is closely related to many interesting phenomena.

Orbital magnetic moments of  $3d$  transition metals are generally quenched because of the crystal field. Some  $3d$  transition-metal oxides exhibit large unquenched orbital magnetic moments, which arise mainly from spin-orbit interaction in the localized  $3d$  orbital, whereby the atomic field is deformed in a relatively slight manner by the crystal field. A strong Coulomb repulsion of  $3d$  electrons might localize  $3d$  orbitals, and reduce the ligand field on the metal atoms, leading to large unquenched orbital moments.<sup>2,3</sup> For instance, results of magnetic x-ray scattering indicate that the orbital magnetic moment of NiO is rather large.<sup>4</sup>

CrO<sub>2</sub>, a potentially important material for future spintronics, is a half-metallic ferromagnet in which one spin channel is conductive but the other one is insulating.<sup>5</sup> As a consequence of the half-metallic feature, the occupied  $3d$  bands of Cr in CrO<sub>2</sub> are fully spin polarized, leading to an integral spin moment of  $2.0\mu_B/\text{CrO}_2$ . Band-structure calculations<sup>6-9</sup> and recent spin-resolved x-ray absorption studies<sup>10</sup> showed that O  $2p$  states in the vicinity of the Fermi level are highly spin polarized. These states are related to the conduction and magnetic properties of CrO<sub>2</sub>. Polarization-dependent x-ray absorption spectroscopy (XAS) measurements showed that Cr  $3d$  states above the Fermi level exhibit a strong anisotropy of orbital occupation.<sup>11</sup> Exploring the orbital contribu-

tion of O and Cr to the magnetic moments of CrO<sub>2</sub> can thus unravel its underlying magnetic properties.

Several experimental techniques, such as neutron scattering, magnetic x-ray scattering, and magnetic circular dichroism (MCD) in XAS, are useful in studying the orbital magnetic moments of materials. Through a modeling of the electronic configuration, it is possible to probe spin and orbital moments separately from neutron scattering data. This separation of spin and orbital magnetization can also be achieved by magnetic x-ray scattering with the help of different prefactors of spin and orbital moment densities.<sup>4,12</sup> MCD in x-ray absorption provides a powerful experimental method to deduce element-specific orbital and spin magnetic moments by means of sum rules. MCD sum rules specify the relation of spin and orbital moments to integrated XAS and integrated MCD spectra.<sup>13-16</sup> For example, the orbital and spin magnetic moments of Fe and Co obtained on applying MCD sum rules to high resolution  $L_{2,3}$ -edge XAS and MCD data agree well with those obtained from Einstein-de Haas gyromagnetic ratio measurements.<sup>17</sup>

In this paper, we present measurements of MCD in soft x-ray absorption and band-structure calculations based on the local spin density approximation with on-site Coulomb energy  $U$  taken into account (LSDA+U) to investigate the orbital magnetic moments of Cr and O in epitaxial CrO<sub>2</sub> thin films grown on TiO<sub>2</sub>(100) substrates. Both our MCD measurements and LSDA+U calculations reveal that O  $2p$  and Cr  $3d$  orbitals are strongly hybridized. We also discuss magnetic coupling between O and Cr, and the effect of  $U$  on the individual orbital and spin magnetic moments.

We carried out MCD measurements in soft x-ray absorption with the elliptically polarized undulator (EPU) beamline of the Synchrotron Radiation Research Center in Taiwan.<sup>18,19</sup> The EPU can generate circularly polarized light or linearly polarized light with the polarization in the horizontal or vertical direction with respect to the storage ring. All soft x-ray absorption measurements were taken with photons of an energy resolution 0.2 eV and a degree of circular polarization 60%. The incident angle was 45° off the sample normal, and

the incident light was in the plane defined by the sample normal and the  $c$  axis. During the measurements,  $\text{CrO}_2$  films were at the magnetically remanent state and kept at a temperature of 80 K. The sample drain current was detected as the absorption signal. MCD spectra were recorded on reversing the remanent magnetization at every photon energy.

High-quality epitaxial  $\text{CrO}_2$  films were grown on  $\text{TiO}_2(100)$  substrates by chemical vapor deposition.<sup>20</sup> The substrates were ultrasonically cleaned with acetone, 1,1,1-trichloroethane, 10% hydrofluoric acid, and distilled water before air drying. The deposition was at 400 °C by using  $\text{CrO}_3$  as the precursor. X-ray diffraction revealed that  $\text{CrO}_2$  films were single crystalline and epitaxial; measurements of the magneto-optical Kerr effect showed a square magnetic hysteresis loop, indicating a high magnetic remanence of the films. Details of the sample preparation and characterization will be published elsewhere.<sup>21</sup>

Self-consistent band-structure calculations including spin-orbit coupling within the LSDA and LSDA+U (Ref. 22) schemes have been performed by using the all-electron full-potential linearized muffin-tin orbital (FP-LMTO) method.<sup>23</sup> The Vosko-Wilk-Nusair<sup>24</sup> exchange-correlation potential and the experimental lattice parameters  $a=4.419$  Å,  $c=2.912$  Å, and  $u=0.303$  of the rutile structure of  $\text{CrO}_2$  were used in the calculations.<sup>25</sup> The radii of the muffin-tin spheres for Cr and O were  $2.0a_0$  and  $1.5a_0$ , respectively, where  $a_0$  is the Bohr radius. The LMTO basis set was expanded in spherical harmonics up to an angular momentum  $l=6$ . The number of  $k$  points used in the self-consistent calculations was 126 over the irreducible wedge of the tetragonal Brillouin zone. To examine the effects of the on-site Coulomb energy  $U$  on the orbital moment, different  $U$ 's from 0 to 6 eV were used in the LSDA+U calculations with the exchange interaction parameter  $J$  kept at 0.87 eV.<sup>8</sup>

The MCD sum rules for orbital moments were independently derived from a localized model<sup>13</sup> and from an itinerant approach<sup>15,16</sup> such as relativistic multiple-scattering theory.<sup>16</sup> Calculations on the basis of a tight-binding approximation show that  $K$ -edge MCD spectra is generated mainly by the  $3d$  orbital moment on the neighboring sites through the  $p$ - $d$  hybridization.<sup>26</sup> MCD spectra of an  $s$ -level absorption reflect the  $p$ -projected orbital magnetization density of unoccupied states. According to x-ray MCD sum rules, orbital magnetic moments  $\mu_{orb}$  in units of  $\mu_B/\text{atom}$  can be obtained from  $K$ -edge XAS and MCD spectra. Sum rules of the  $K$ -edge absorption relate orbital magnetic moments to  $K$ -edge XAS and MCD spectra as<sup>13,15,16</sup>

$$\mu_{orb} = -\frac{2}{3} \frac{\int_K (\mu_+ - \mu_-) d\omega}{\int_K (\mu_+ + \mu_-) d\omega} (6 - n_p), \quad (1)$$

where  $n_p$  and  $\omega$  are the electron occupation number in the  $2p$  states and the photon energy, respectively;  $\mu_+$  and  $\mu_-$  are cross sections for absorption taken with the projection of the spin of the incident photons parallel and antiparallel to

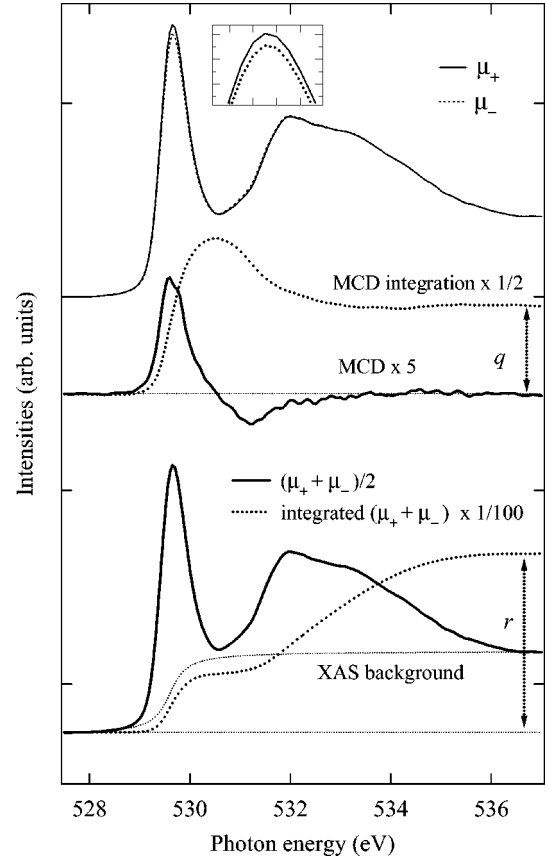


FIG. 1.  $K$ -edge XAS and MCD spectra of O in  $\text{CrO}_2$ . Top panel: XAS spectra with spin of photons parallel (denoted as  $\mu_+$ ) and anti-parallel (denoted as  $\mu_-$ ) to that of Cr  $3d$  majority electrons, respectively. Middle panel: MCD, i.e.,  $(\mu_+ - \mu_-)/[\cos 45^\circ \times 0.6]$ , and MCD integration of the O  $K$ -edge absorption. Bottom panel: XAS integration spectra with an XAS background (thin broken line). The  $r$  and  $q$  denote the integration of XAS and MCD spectra across the  $K$  edge, respectively.

the spin of the majority electrons in transition metals, respectively.  $K$  denotes the integration range across the  $K$  edge of the spectra.

Figure 1 presents the O  $K$ -edge XAS and MCD of  $\text{CrO}_2$ . After correction for the incomplete polarization and the incident angle of soft x ray, i.e., multiplying  $(\mu_+ - \mu_-)$  by  $1/[\cos 45^\circ \times 0.6]$  for MCD spectra while keeping XAS  $= (\mu_+ + \mu_-)$  unchanged, we found that the MCD to XAS ratio at the pre-peak position of O  $K$ -edge absorption is 4.1%, which is larger than that, 3%, observed on  $\text{La}_{1-x}\text{Sr}_x\text{MnO}_3$  single crystals.<sup>27</sup> For  $q$  and  $r$  as the integrated intensities of MCD and XAS spectra across the  $K$  edge, the orbital magnetic moment per O atom is  $\mu_{orb} = -\frac{2}{3}(q/r)(6 - n_p)$ . To quantitatively obtain the O  $2p$  hole density, we compare the spectrum of O  $1s$  XAS of  $\text{CrO}_2$  with that of  $\text{O}_2$  molecules, as shown in Fig. 2, in which the XAS intensity of  $\text{CrO}_2$  at a photon energy of 560 eV is normalized to that of  $\text{O}_2$ . To a first-order approximation, the integrated prepeak intensity of O  $1s$  XAS is proportional to the average number of O  $2p$  holes per atom. The integration of the prepeak intensity of O  $1s$  XAS of  $\text{CrO}_2$  is 25% of that of  $\text{O}_2$ , which has two well-defined  $2p$  holes per atom. The average number of O  $2p$

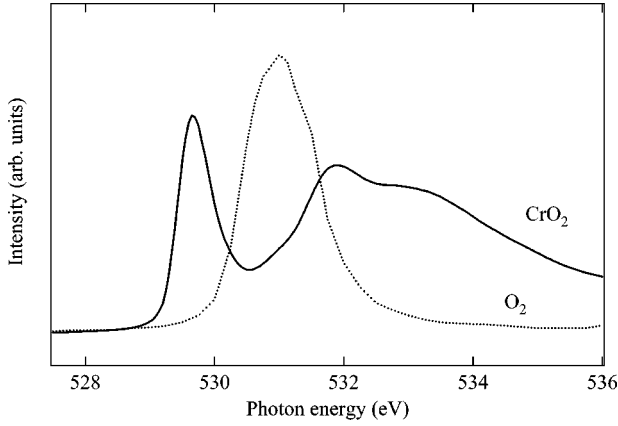


FIG. 2. Isotropic O  $1s$  XAS spectra (thick lines) of  $\text{CrO}_2$  (taken as the 1:2 weighted average of  $\mathbf{E}\parallel c$  and  $\mathbf{E}\perp c$  spectra) and  $\text{O}_2$  (after Ref. 28).

holes per atom in  $\text{CrO}_2$  is estimated to be 0.5. With an arctangentlike edge-jump function for the background of the XAS spectra, the O orbital magnetic moment is therefore estimated to be  $-(0.003 \pm 0.001)\mu_B$ . The large uncertainty originates mainly from our estimate of the number of O  $2p$  holes, the background functions of XAS spectra, and the uncertainty from the degree of circular polarization of incident photons.

With x-ray MCD sum rules,  $L_{2,3}$ -edge XAS and MCD spectra also provide information on the orbital magnetic moment of transition metals as in the equation

$$\mu_{orb} = -\frac{4}{3} \frac{\int_{L_{2,3}} (\mu_+ - \mu_-) d\omega}{\int_{L_{2,3}} (\mu_+ + \mu_-) d\omega} (10 - n_d), \quad (2)$$

where  $n_d$  is the  $3d$  electron occupation number of transition metals.  $L_{2,3}$  denotes the integration range across  $L_2$  and  $L_3$  absorption edges. Figure 3 displays the Cr  $L$ -edge XAS and MCD spectra of  $\text{CrO}_2$ . For  $q$  and  $r$  as the integrated intensities of MCD and XAS spectra across the  $L_{2,3}$  edges, respectively, as shown in Fig. 3, the orbital magnetic moment of Cr is  $\mu_{orb} = -\frac{4}{3}(q/r)(10 - n_d)$ . With an appropriate arctangentlike edge-jump function for the XAS background and  $n_d \sim 1$ ,<sup>29</sup> our MCD data indicate that the orbital magnetic moment of Cr is  $-(0.06 \pm 0.02)\mu_B$ . In our measurements, saturation effects have been corrected on normalizing the XAS spectra to the normal incidence data, because MCD data obtained in the electron yield mode might yield an incorrect value of the orbital moment caused by saturation effects.<sup>30</sup> In contrast, our MCD and XAS data do not provide quantitative information on the spin moment of Cr, because one cannot uniquely define which part of the spectra belongs to the  $L_3$  or  $L_2$  edges. This is due to the large multiplet splitting in the XAS final states relative to the Cr  $2p$  core-level spin-orbit splitting. Nevertheless, the integration spectrum of our MCD data indicates that the orbital moment of Cr is opposite to its spin moment, since that the sign of spin moment is determined by<sup>14</sup>

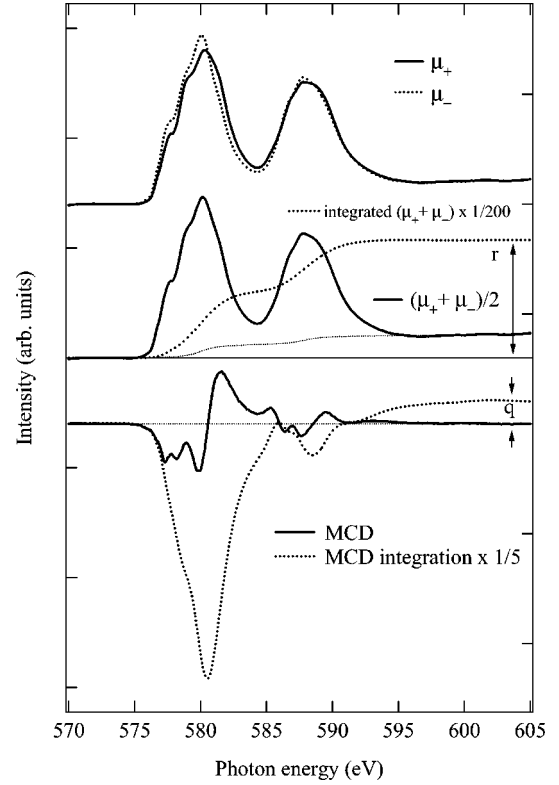


FIG. 3.  $L_{2,3}$ -edge XAS and MCD spectra of Cr in  $\text{CrO}_2$ . Top panel: XAS spectra with incident photon of different spin directions. Middle panel: XAS integration spectra with an arctangentlike edge-jump function of background (thin broken line). Bottom panel: MCD and MCD integration spectra. The descriptions of the figure correspond to those of Fig. 1.

$$-6 \int_{L_3} (\mu_+ - \mu_-) d\omega + 4 \int_{L_{2,3}} (\mu_+ - \mu_-) d\omega, \quad (3)$$

in which the first integration is negative and the second integration is positive.

Quantitative orbital moments obtained by MCD and XAS measurements depend strongly on the background function of XAS and the electron occupation numbers in O  $2p$  and Cr  $3d$  valence bands. It should be noted that accurately pinning down the value of orbital moments using MCD data is far from being trivial. MCD measurements presented above, nevertheless, provide valuable qualitative information on element specific orbital magnetic moment. Our measurements reveal that the Cr orbital moments of  $\text{CrO}_2$  are opposite to its spin moment, but are aligned parallel to the O orbital moment.

To study further the magnetic moments of Cr and O in  $\text{CrO}_2$ , we performed band-structure calculations in LSDA and LSDA+U schemes. The calculated spin and orbital magnetic moments of O and Cr in units of  $\mu_B/\text{atom}$  are summarized in Table I. The antialignment between spin moments of Cr and O results from a charge transfer of O  $2p$  to Cr  $3d$ , so producing O  $2p$  electrons with negative net spin moments. Our calculated orbital and spin moments of Cr are antiparallel, consistent with Hund's rule coupling for a  $3d$  shell which is less than half full. Interestingly, MCD mea-

TABLE I. Calculated spin ( $\mu_{spin}$ ) and orbital ( $\mu_{orb}$ ) magnetic moments of O and Cr in CrO<sub>2</sub> in units of  $\mu_B$ /atom with the exchange interaction parameter  $J=0.87$  eV. The Coulomb interaction energy  $U$  is in units of eV.

|    | $U$          | 0       | 2       | 3       | 4       | 6       |
|----|--------------|---------|---------|---------|---------|---------|
| O  | $\mu_{spin}$ | -0.042  | -0.058  | -0.079  | -0.094  | -0.11   |
|    | $\mu_{orb}$  | -0.0012 | -0.0019 | -0.0025 | -0.0030 | -0.0042 |
| Cr | $\mu_{spin}$ | 1.89    | 1.94    | 1.99    | 2.03    | 2.08    |
|    | $\mu_{orb}$  | -0.037  | -0.046  | -0.051  | -0.056  | -0.069  |

measurements and calculations lead to the Cr orbital moment being parallel to that of O. One can extend Hund's rule to account for the parallel coupling between the orbital and spin moments of O, resulting in a parallel coupling of orbital moments of Cr and O.

The LSDA ( $U=J=0$ ) calculations give rise to spin and orbital moments of  $1.89\mu_B$  and  $-0.037\mu_B$  per Cr atom, respectively. The magnitudes of spin and orbital magnetic moments are enhanced as the on-site Cr  $3d$ - $3d$  Coulomb interaction increases.<sup>31</sup> The influence of  $U$  on the spin magnetic moments of CrO<sub>2</sub> can be understood as follows. Conceptually, the shift of Cr  $3d$  spin-up density of state slightly away from the Fermi level increases the Cr spin moment. With the inclusion of on-site Coulomb interaction  $U$ , the Cr  $3d$  conduction band is pushed downward in energy, and charge transfer from O  $2p$  spin-up electrons to Cr  $3d$  electrons is increased, leading to an increased spin moment of Cr. Such an enhancement of charge transfer also increases the O spin moment. When  $U$  is 3–4 eV, the spin moment of Cr is close

to  $2.0\mu_B$ , the value predicted by Hund's rules for the spin moment of a Cr<sup>4+</sup> ion. In addition, the enhancement of the orbital magnetic moment with the increase of  $U$  is also consistent with the unquenched orbital moments of CoO and NiO in which the Coulomb interaction dominates the orbital magnetism.<sup>2,3</sup> Comparing with the LSDA+ $U$  calculations and MCD measurements, we deduce that the on-site Coulomb interaction energy of CrO<sub>2</sub> is 3–4 eV, in satisfactory agreement with previous LSDA+ $U$  work which concluded the on-site Coulomb energy of Cr  $3d$  electrons in CrO<sub>2</sub> to be 3 eV.<sup>8</sup>

To conclude, measurements of MCD in soft x-ray absorption and LSDA+ $U$  calculations have unraveled the orbital contribution of Cr and O to the magnetization of CrO<sub>2</sub>. We found that oxygen atoms in CrO<sub>2</sub> exhibit a significant orbital magnetic moment relative to other oxides. Our results conclude that the orbital magnetic moments of O is coupled parallel to that of Cr, while the spin moments are coupled antiparallel. In addition, the magnitudes of spin and orbital magnetic moments are enhanced as the on-site Cr  $3d$ - $3d$  Coulomb interaction increases. Comparing the MCD data with the LSDA+ $U$  calculations, we conclude that it is essential to include the on-site Coulomb energy for adequately describing the orbital magnetic moments of CrO<sub>2</sub>.

The authors thank L. H. Tjeng and C. S. Hsue for discussions. C. C. Wu was supported by a postdoctoral fellowship of the Academia Sinica. This work was supported in part by the National Science Council of Taiwan (NSC90-2112-M-213-002, NSC90-2119-M-007-004 and NSC90-2112-M-002-040).

- <sup>1</sup>M. Imada, A. Fujimori, and Y. Tokura, *Rev. Mod. Phys.* **70**, 1039 (1998).
- <sup>2</sup>I. V. Solov'ev, A. I. Liechtenstein, and K. Terakura, *Phys. Rev. Lett.* **80**, 5758 (1998).
- <sup>3</sup>S. K. Kwon and B. I. Min, *Phys. Rev. B* **62**, 73 (2000).
- <sup>4</sup>V. Fernandez, C. Vettier, F. de Bergevin, C. Giles, and W. Neubeck, *Phys. Rev. B* **57**, 7870 (1998).
- <sup>5</sup>R. A. de Groot, F. M. Mueller, P. G. van Engen, and K. H. J. Buschow, *Phys. Rev. Lett.* **50**, 2024 (1983).
- <sup>6</sup>K. Schwarz, *J. Phys. F: Met. Phys.* **16**, L211 (1986).
- <sup>7</sup>S. P. Lewis, P. B. Allen, and T. Sasaki, *Phys. Rev. B* **55**, 10253 (1997).
- <sup>8</sup>M. A. Korotin, V. I. Anisimov, D. I. Khomskii, and G. A. Sawatzky, *Phys. Rev. Lett.* **80**, 4305 (1998).
- <sup>9</sup>I. I. Mazin, D. J. Singh, and C. A. Draxl, *Phys. Rev. B* **59**, 411 (1999).
- <sup>10</sup>D. J. Huang, L. H. Tjeng, J. Chen, C. F. Chang, W. P. Wu, A. D. Rata, T. Hibma, S. C. Chung, S.-G. Shyu, C.-C. Wu, and C. T. Chen, *Surf. Rev. Lett.* **9**, 1007 (2002).
- <sup>11</sup>C. B. Stagarescu, X. Su, D. E. Eastman, K. N. Altmann, F. J. Himpsel, and A. Gupta, *Phys. Rev. B* **61**, R9233 (2000).
- <sup>12</sup>M. Blume and D. Gibbs, *Phys. Rev. B* **37**, 1779 (1988).
- <sup>13</sup>B. T. Thole, P. Carra, F. Sette, and G. van der Laan, *Phys. Rev. Lett.* **68**, 1943 (1992).
- <sup>14</sup>P. Carra, B. T. Thole, M. Altarelli, and X. Wang, *Phys. Rev. Lett.* **70**, 694 (1993).
- <sup>15</sup>A. Ankudinov and J. J. Rehr, *Phys. Rev. B* **51**, 1282 (1995).
- <sup>16</sup>G. Y. Guo, *Phys. Rev. B* **57**, 10295 (1998).
- <sup>17</sup>C. T. Chen, Y. U. Idzerda, H.-J. Lin, N. V. Smith, G. Meigs, E. Chaban, G. H. Ho, E. Pellegrin, and F. Sette, *Phys. Rev. Lett.* **75**, 152 (1995).
- <sup>18</sup>C. S. Hwang and S. Yeh, *Nucl. Instrum. Methods Phys. Res. A* **420**, 29 (1999).
- <sup>19</sup>S.-C. Chung, J. Chen, L.-R. Huang, R. T. Wu, C.-C. Chen, N.-F. Cheng, J. M. Chuang, P.-C. Tseng, D.-J. Huang, C. F. Chang, S.-Y. Perng, C. T. Chen, K.-L. Tsang, *Nucl. Instrum. Methods Phys. Res. A* **467-478**, 445 (2001).
- <sup>20</sup>X. W. Li, A. Gupta, and Giang Xiao, *Appl. Phys. Lett.* **75**, 713 (1999).
- <sup>21</sup>S. G. Shyu *et al.* (unpublished).
- <sup>22</sup>A. I. Liechtenstein, V. I. Anisimov, and J. Zaanen, *Phys. Rev. B* **52**, R5467 (1995).
- <sup>23</sup>S. Y. Savrasov, *Phys. Rev. B* **54**, 16470 (1996).
- <sup>24</sup>S. H. Vosko, L. Wilk, and M. Nusair, *Can. J. Phys.* **58**, 1200 (1980).
- <sup>25</sup>P. Porta, M. Marezio, J. P. Remeika, and P. D. Dernier, *Mater. Res. Bull.* **7**, 157 (1972).

<sup>26</sup>J. Igarashi and K. Hirai, Phys. Rev. B **50**, 17 820 (1994).

<sup>27</sup>E. Pellegrin, H. J. Tjeng, F. M. de Groot, R. Hesper, G. A. Sawatzky, Y. Moritomo, and Y. Tokura, J. Electron Spectrosc. Relat. Phenom. **86**, 115 (1997).

<sup>28</sup>Y. Ma, C. T. Chen, G. Meigs, K. Randall, and F. Sette, Phys. Rev. A **44**, 1848 (1991).

<sup>29</sup>Since there is one hole in the O  $2p$  bands per formula unit and the energy bands crossing the Fermi level are dominated by O  $2p$

bands, one can estimate that the average number of the  $3d$  electrons per Cr atom is  $\sim 1$ .

<sup>30</sup>R. Nakajima, J. Stohr, and Y. U. Idzerda, Phys. Rev. B **59**, 6421 (1999).

<sup>31</sup>For all values of  $U$ , total spin moments per formula unit remain  $2.0\mu_B$  if those of the interstitial region are included, consistent with the half-metallic feature of  $\text{CrO}_2$ .